



AFRL-RX-WP-TP-2011-4374

**THE INFLUENCE OF MICROSTRUCTURE AND
MICROTEXTURE ON FATIGUE CRACK INITIATION
AND GROWTH IN $\alpha + \beta$ TITANIUM (PREPRINT)**

**Adam L. Pilchak and Andrew H. Rosenberger
Metals Branch**

**Kazuo Nakase
Sumikin Kansai Industries Ltd.**

**Ikuhiro Inagaki and Yoshihisa Shirai
Sumitomo Metal Industries, Ltd.**

**James C. Williams
Ohio State University**

OCTOBER 2011

Approved for public release; distribution unlimited.

See additional restrictions described on inside pages

STINFO COPY

**AIR FORCE RESEARCH LABORATORY
MATERIALS AND MANUFACTURING DIRECTORATE
WRIGHT-PATTERSON AIR FORCE BASE, OH 45433-7750
AIR FORCE MATERIEL COMMAND
UNITED STATES AIR FORCE**

REPORT DOCUMENTATION PAGE					Form Approved OMB No. 0704-0188	
The public reporting burden for this collection of information is estimated to average 1 hour per response, including the time for reviewing instructions, searching existing data sources, gathering and maintaining the data needed, and completing and reviewing the collection of information. Send comments regarding this burden estimate or any other aspect of this collection of information, including suggestions for reducing this burden, to Department of Defense, Washington Headquarters Services, Directorate for Information Operations and Reports (0704-0188), 1215 Jefferson Davis Highway, Suite 1204, Arlington, VA 22202-4302. Respondents should be aware that notwithstanding any other provision of law, no person shall be subject to any penalty for failing to comply with a collection of information if it does not display a currently valid OMB control number. PLEASE DO NOT RETURN YOUR FORM TO THE ABOVE ADDRESS.						
1. REPORT DATE (DD-MM-YY) October 2011		2. REPORT TYPE Technical Paper		3. DATES COVERED (From - To) 1 October 2011 – 1 October 2011		
4. TITLE AND SUBTITLE THE INFLUENCE OF MICROSTRUCTURE AND MICROTTEXTURE ON FATIGUE CRACK INITIATION AND GROWTH IN $\alpha + \beta$ TITANIUM (PREPRINT)				5a. CONTRACT NUMBER In-house		
				5b. GRANT NUMBER		
				5c. PROGRAM ELEMENT NUMBER 62102F		
6. AUTHOR(S) Adam L. Pilchak and Andrew H. Rosenberger (Metals Branch) Kazuo Nakase (Sumikin Kansai Industries Ltd.) Ikuhiro Inagaki and Yoshihisa Shirai (Sumitomo Metal Industries, Ltd.) James C. Williams (Ohio State University)				5d. PROJECT NUMBER 4347		
				5e. TASK NUMBER 20		
				5f. WORK UNIT NUMBER LM121100		
7. PERFORMING ORGANIZATION NAME(S) AND ADDRESS(ES) <div style="display: flex; justify-content: space-between;"> <div style="width: 45%;"> Metals Branch/Metals, Ceramics & Nondestructive Evaluation Division Air Force Research Laboratory, Materials and Manufacturing Directorate Wright-Patterson Air Force Base, OH 45433-7750 Air Force Materiel Command, United States Air Force </div> <div style="width: 45%;"> Sumikin Kansai Industries Ltd. Osaka, Japan Sumitomo Metal Industries, Ltd, Osaka Japan Sumitomo Metal Industries, Ltd, Hyogo, Japan Ohio State University, Columbus, Ohio </div> </div>				8. PERFORMING ORGANIZATION REPORT NUMBER AFRL-RX-WP-TP-2011-4374		
9. SPONSORING/MONITORING AGENCY NAME(S) AND ADDRESS(ES) Air Force Research Laboratory Materials and Manufacturing Directorate Wright-Patterson Air Force Base, OH 45433-7750 Air Force Materiel Command United States Air Force				10. SPONSORING/MONITORING AGENCY ACRONYM(S) AFRL/RXLM		
				11. SPONSORING/MONITORING AGENCY REPORT NUMBER(S) AFRL-RX-WP-TP-2011-4374		
12. DISTRIBUTION/AVAILABILITY STATEMENT Approved for public release; distribution unlimited.						
13. SUPPLEMENTARY NOTES The U.S. Government is joint author of this work and has the right to use, modify, reproduce, release, perform, display or disclose the work. PA Case Number and clearance date: 88ABW-2011-2002, 21Apr 2011. Preprint journal article to be submitted to 12 th Int'l conference on Titanium. This document contains color.						
14. ABSTRACT The strain paths and thermal cycles utilized during thermomechanical processing of two-phase alloys have a pronounced influence on the resulting distribution of grain orientations present and their spatial distribution. For example, large regions of similarly oriented α grains, commonly referred to as microtextured regions or macrozones, may persist despite the imposition of large macroscopic strains. The detrimental effect of microtexture on dwell fatigue life of high temperature alloys is well established; however, considerably less attention has been given to the effects of microtexture on fatigue life during continuous cycling. In the present work, the effects of microstructure and microtexture on the low cycle fatigue ($N_f \leq 10^4$ cycles) behavior of Ti-6Al-4V have been characterized using electron microscopy. Microstructural parameters such as the volume fraction and size of the α phase were assessed by quantitative metallography while the contiguity of the α phase and the size and shape of the microtextured regions were investigated with electron backscatter diffraction.						
15. SUBJECT TERMS fatigue, crack initiation, crack growth, microstructure, EBSD, fractography						
16. SECURITY CLASSIFICATION OF:			17. LIMITATION OF ABSTRACT: SAR	NUMBER OF PAGES 6	19a. NAME OF RESPONSIBLE PERSON (Monitor) Andrew Rosenberger	
a. REPORT Unclassified	b. ABSTRACT Unclassified	c. THIS PAGE Unclassified			19b. TELEPHONE NUMBER (Include Area Code) N/A	

The influence of microstructure and microtexture on fatigue crack initiation and growth in $\alpha + \beta$ titanium

Adam L. Pilchak¹, Kazuo Nakase², Ikuhiro Inagaki³, Yoshihisa Shirai⁴, Andrew H. Rosenberger¹ and James C. Williams⁵

¹ Air Force Research Laboratory, Materials and Manufacturing Directorate, AFRL/RXLM, Wright Patterson AFB OH 45433

² Sumikin Kansai Industries, Ltd., Osaka 554-0024 Japan

³ Sumitomo Metal Industries, Ltd., Titanium Alloy Engineering Section, Osaka 554-0024 Japan

⁴ Sumitomo Metal Industries, Ltd., Stainless Steel & Titanium Research and Development Department, Hyogo 660-0891 Japan

⁵ The Ohio State University, Columbus, OH 43210 USA

The strain paths and thermal cycles utilized during thermomechanical processing of two-phase alloys have a pronounced influence on the resulting distribution of grain orientations present and their spatial distribution. For example, large regions of similarly oriented α grains, commonly referred to as microtextured regions or macrozones, may persist despite the imposition of large macroscopic strains. The detrimental effect of microtexture on dwell fatigue life of high temperature alloys is well established; however, considerably less attention has been given to the effects of microtexture on fatigue life during continuous cycling. In the present work, the effects of microstructure and microtexture on the low cycle fatigue ($N_f \leq 10^4$ cycles) behavior of Ti-6Al-4V have been characterized using electron microscopy. Microstructural parameters such as the volume fraction and size of the α phase were assessed by quantitative metallography while the contiguity of the α phase and the size and shape of the microtextured regions were investigated with electron backscatter diffraction. Variations in microstructure and microtexture due to subtle differences in thermomechanical processing routes have been correlated with variations in fatigue life through the use of quantitative fractography techniques. Using these methods the spatial and crystallographic orientations of fracture facets at small crack lengths have been determined. The results indicate that grains with c -axes are oriented between approximately 25° and 55° from the stress axis are most likely to form cracks that propagate by facet formation on the basal plane. Crack advance by faceted growth occurs readily through grains with similar basal plane orientation and, as a result, the contiguity of equiaxed α grains with basal poles in the $25^\circ - 55^\circ$ range is an important parameter governing low cycle fatigue life.

Keywords: fatigue, crack initiation, crack growth, microstructure, EBSD, fractography

1. Introduction

Two-phase titanium alloys have the unique characteristic that regions of similar crystallographic orientation, known as either microtextured regions or macrozones, persist through large strains during thermomechanical processing (TMP)¹. The presence^{2,3} of microtextured regions has been shown to cause a substantial reduction in fatigue life when a hold at peak stress, or dwell period, is imposed. Although multiple cracks form during dwell fatigue loading, the critical crack seems to grow from the largest of these regions⁵. The sample volume and shape of microtextured regions⁶ have recently been implicated in dwell fatigue life variability in laboratory specimens making the development of transfer functions for components difficult. Modeling efforts⁷⁻¹⁰ have revealed the effects of microtexture at the grain level in creating non-uniform stress-strain distributions, the accumulation of plastic slip near grain boundaries and the propensity for crack nucleation.

However, considerably less attention has been given to the effects of microtexture on ordinary continuous cycling fatigue life. Several studies have confirmed the crystallographic nature of small and near-threshold crack growth at low ΔK ^{5,11} and it is agreed that crack growth during cyclic loading occurs on the basal plane, presumably along pre-existing slip bands. There have been limited experimental measurements of the spatial orientations of fracture facets as a function of loading history^{5,6}, but it is clear that cyclic facet formation tends to occur on high Schmid Factor planes inclined to the loading direction. At small crack lengths, the presence of microtexture has been shown to support extended faceted growth over longer distances in the microstructure

compared to material with randomly oriented grains¹². At longer crack lengths, Bowen¹³ showed that long crack growth rates were significantly affected by crystallographic orientation in strongly textured plate. The change in crack growth rates were correlated with changes in fracture mode and topography. Bantounas et al.¹⁴ have shown that fatigue crack growth occurs by different mechanisms in microtextured regions of different orientation. Regions oriented for easy prismatic $\langle a \rangle$ slip supported crack extension by striation growth whereas regions oriented for pyramidal $\langle c+a \rangle$ slip tended to fail by mechanisms resembling monotonic loading fracture. It follows that significant variation in crack growth rate would be expected in microtextured material. Because low cycle fatigue is predominantly crack-growth controlled, it would be expected that microtexture would exert a strong influence on fatigue behavior as it has been shown to affect the small and long crack regimes.

While carefully designed TMP schedules can reduce the extent of microtexture formation^{1,15,16}, it is almost inevitable that there will be some clusters of similarly oriented grains in a final forged component. These statistical weak-links can be easily discovered by fatigue testing, however, it would be useful to rank the resistance of a particular microstructure to its fatigue crack growth resistance. In the present work, we present a methodology for this purpose that correlates, microstructure including microtexture as affected by processing history with properties, particularly low cycle fatigue.

2. Materials and Experimental Procedure

The material selected for this work was Ti-6Al-4V. The alloy was cast as production-scale, cylindrical ingots

Table 1. Summary of microstructural features and properties. *Loading axis transverse to bar axis.

Sample	Route	α particle size (max α particle size), μm	V_f primary α	0.2% σ_y , MPa	UTS, MPa	Elongation/ RA, %	Cycles to failure
¹ FE1	E2a	7.9 \pm 6.2 (43.9)	0.65	861	960	18.8 / 41.9	416,615
⁵ GKT(L) *	E2a	6.3 \pm 3.8 (29.0)	0.62	884	979	16.8 / 37.4	46,124
³ LRL	L2b	7.9 \pm 5.8 (42.1)	0.67	881	975	16.9 / 37.2	98,104
⁴ MGT	M1c	6.8 \pm 4.2 (34.1)	0.63	886	979	14.4 / 33.2	65,803
² AL93	U	8.2 \pm 6.0 (43.5)	0.61	870	968	16.3 / 41.3	206,516

Comment [R11]: note that these will be changed to arbitrary letters once completed, they are left here for my reference right now.

Comment [rev12]: Also note this (L) is for our purposes only and will be removed

with sizes up to 280 mm in diameter. The coarse, columnar ingot structure was refined through a series of TMP steps that included $\alpha + \beta$ forging and $\alpha + \beta$ finishing steps to produce production-scale bar. A total of three processing routes were used to prepare material for the present work; however, details of the processing sequences are proprietary and for the purpose of this paper the effects of different processing routes on fatigue behavior is the important point. For simplicity, samples are subsequently identified by the letters A, B and C to distinguish between processing routes.

Strain-control LCF tests, with a constant strain amplitude of 0.71%, were performed on a servo hydraulic test frame at 93 °C (~200 °F). For the purposes of this paper, one representative longitudinal fatigue sample is used from each processing route. In addition, a transverse fatigue specimen was tested from route A and a sample with completely unknown processing history was tested (route U). The as-fractured specimens were protected with an acrylic lacquer and sectioned perpendicular to the loading direction. The lacquer was later removed with acetone and the fracture surfaces were investigated in a scanning electron microscope (SEM).

The sample microstructures were characterized by light metallography and scanning electron microscopy. Quantitative metallography was used to determine the size and volume fraction of primary α particles. The results are shown in Table 1. The extent of micro- and macrotexture was investigated via EBSD using a SEM equipped with a field emission gun. The samples used for EBSD analysis were sectioned with the longitudinal direction of the gauge section of the fatigue samples (containing the loading direction in the plane of polish). For the EBSD experiments, the SEM was operated at an accelerating voltage of 20 kV with a probe current of approximately 10.5 nA at a working distance of 25 mm. The scanned areas were typically of the order of 4 ~ 8 mm² at resolutions of 1.5 – 2.5 μm .

3. Results and Discussion

3.1 Microstructure and Texture

The microstructure resulting from the three thermomechanical processing sequences were all typical of $\alpha + \beta$ worked material consisting of globular α particles in a matrix of transformed β . The microstructure was characterized to determine the volume fraction of primary α particles, the mean and standard deviation of the α particle size and the maximum α particle size. The

size measurements were made using the line intercept method. The results are summarized in Table 1. A comparison of the three processing routes reveals no substantial variations among the routes in the volume fraction of primary α despite +/- 100 °C variations in finishing temperature. The mean α particle sizes were similar among all samples, all being significantly less than one standard deviation from one another. The maximum particle size, varied somewhat more, but was still relatively small.

The macrotexture of the samples, as determined by reduction of EBSD data were collected from large areas. At first inspection, the textures seem considerably different, but considering that the stress state is uniaxial and axisymmetric, they are actually quite similar. In general, except for FE1, all of the samples have similar macrotexture with basal poles oriented at all angles between 0 and 90° to the loading direction, although subtle variations in intensity were noted. For example, samples LRL and AL93 have highest intensities along the loading direction, while samples GKT and MGT have slightly higher intensities where [0001] is inclined to the tensile axis. In contrast, sample FE1 was in an elastically and plastically soft orientation with [10 $\bar{1}$ 0] oriented along the tensile direction.

3.2 Microstructure-Property Correlations

In this section we present the properties of the five conditions and subsequently discuss the relation between the microstructure, which includes microtexture, and LCF life. The room temperature tensile properties and LCF lives of the various conditions are shown in Table 1. A quick comparison reveals that LCF life does not correlate with yield strength, σ_y , ultimate tensile strength or ductility. These data show a large variation in fatigue behavior as affected by processing history even though the microstructures as determined by conventional methods are ostensibly the same. Fractographic examination showed that fatigue crack initiation and the early stages of crack growth occurred by facet formation. It has been shown^{5,6)} that these facets lie on (0001) and form in grains oriented to favor a type slip on the basal plane. The crack propagation mode transitioned to classic striation formation for all samples at crack lengths of ~ 1 mm. Representative fractographs of these propagation modes are shown in Figure 1 (a) and (b). A qualitative correlation was found between the size / shape of the faceted region and LCF life. In general, samples exhibiting more extensive faceted growth had lower lives,

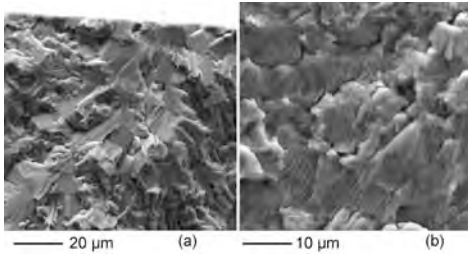


Figure 1. Examples of (a) faceted and (b) striation crack growth in samples LRL and GKT, respectively.

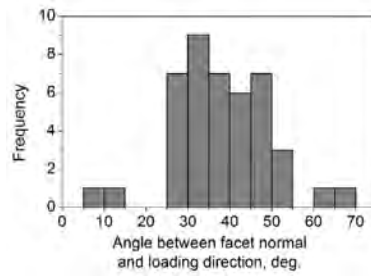


Figure 2. Histogram of facet normal angles (43 measurements).

however, a method for a more quantitative metric for assessing LCF life is desirable.

Previous work¹⁷⁾ has shown that faceted crack growth is faster than striation growth at equivalent driving force. Because much of the total low cycle fatigue life is spent in crack growth, we argue that materials containing a large number of grains favorably oriented for facet formation will naturally have shorter lives. This is especially true in microtextured materials where clusters of similarly oriented grains permit easy crack extension by faceted growth. Such a situation causes the crack to grow rapidly with a concomitant increase in crack driving force which shortens the specimen life. Having established that facet formation is strongly orientation dependent, and that crack growth occurs more rapidly via faceted growth, it is necessary to identify the range of grain orientations that can support faceted growth. For this purpose, we have employed the quantitative tilt fractography (QTF) / EBSD⁵⁾ technique. After confirming that the facets were indeed parallel to (0001) on approximately 10 facets, QTF was used to determine the spatial orientation of another 33 facets to create the distribution of facet normal orientations as shown in Figure 2. Based on this distribution, it is clear that grains with basal poles between approximately 25° and 55° from the loading direction are most likely to initiate and sustain faceted growth.

In order to make a quantitative comparison of the various processing routes, we have characterized the spatial distribution of grain orientations in representative samples with large-scale, automated EBSD. The resulting data were post-processed and segmented to produce a binary image in which the grains capable of sustaining faceted growth (where [0001] is between 25° and 55° from the loading direction) are black while all others remain white. An example of this type of data, termed a 'crystal direction map,' (CDM) is shown in Figure 3. These maps contain two important pieces of information, namely, the fraction of grains oriented for easy facet formation (whether it be initiation or growth) and the spatial distribution of these grains. The former gives information regarding the number of potential nucleation sites while the latter relates to crack propagation resistance. For the case of LCF, which is crack propagation limited, the spatial distribution would be most important factor because it will dictate the amount of time the crack front spends in fast-growing grains.

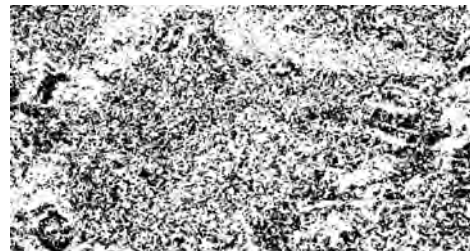


Figure 3. Crystal direction map for sample GKT where black grains have [0001] between 25° and 55° from the loading direction (vertical).

Thus, the following method was used to make a quantitative comparison of the CDMs. Since each map was collected on a longitudinal section of the sample gauge, the loading direction was contained in the plane of polish and, if this section had cracked, the macroscopic crack plane would be nominally perpendicular to the loading direction. Thus, theoretical crack growth paths were traced on the EBSD scans and the distance in which the crack would have been contained within the black (faceted) and white (non-faceted) regions was recorded. This process was repeated in sequence for each row in the EBSD scan and the resulting data was analyzed statistically. Some of the first order results are reported in Table 2. These values capture the general trend of data, but there is usually at least one sample out of place. The one exception is the area fraction of facet forming grains. This parameter scales inversely with LCF life over the range of microstructures investigated here.

For a more quantitative comparison, the data were also represented in cumulative distribution function (CDF) space. Normally distributed axes were used in the plot, Figure 4, to highlight differences in the data. Similar comparisons can be made for the non-faceted regions, which all tended to similar values for the present alloy and are therefore omitted to save space. These plots assume that each data point is uncorrelated and describe the probability that the crack front will be in a faceted (or non-faceted) region of a particular size. Of course larger sizes correlate with both decreased resistance to crack propagation and increases in the driving force for further crack extension. This figure shows a strong correlation between faceted growth and shorter LCF life. The positions of samples MGT and GKT are reversed on the

Table 2. Statistics extracted from crystal direction maps. MFP = mean free path, f = area fraction of facet-forming grains.

Sample	MFP faceted	Max faceted	MFP non-faceted	f
¹ FE1	6.0 ± 5.0	64.5	23.1 ± 27.1	0.20
⁵ GKT-L	9.0 ± 8.4	123.1	15.0 ± 17.5	0.37
³ LRL	9.2 ± 7.1	83.9	20.3 ± 21.7	0.31
⁴ MGT	10.8 ± 9.9	126.1	19.7 ± 23.3	0.35
² AL93	7.8 ± 6.0	59.4	20.3 ± 19.2	0.28

plot from where they might be expected based on a literal ranking of fatigue life. However, the difference in life of these samples is less than 20,000 cycles and may be less than the resolution of this technique. The method is able to accurately separate the order-of-magnitude differences in life, e.g. samples GKT and FE1. Examining the CDF plot (Figure 4) shows that in the shorter life specimens, there is indeed a lower probability that the crack will be in a larger region of facet-forming grains than in the long life specimens. A qualitative check of this result is that there is a strong correlation between large facets seen fractographically and grain clusters seen in the crystal direction map. Since facets form only in the small crack and low- ΔK regimes, this implies that LCF life variability within samples processed via a given route may be caused by differences in the local microstructural neighborhoods where the cracks initiate. This is a point for further research.

This analysis has its limitations, of course, and needs to be explored further. First and foremost is whether or not the sampled area satisfies the requirements to be classified as a representative volume element. Nevertheless, an interesting correlation was observed that warrants further investigation. In addition, while it was reported that faceted growth is up to 10x faster than other modes of growth¹⁷⁾, additional experiments should be performed on samples with controlled microstructure, texture and microtexture and as a function of microstructure.

4 Summary and Conclusion

In this paper we have examined Ti-6Al-4V that has been processed by three different routes and a fourth condition that has been processed by an unknown but still different route. Even though the microstructures as determined by metallography were ostensibly the same, we have shown that the nature and degree of microtexture are quite different. Fractographic examination of failed LCF specimens showed that the cracks initially propagate along basal planes and grains oriented with basal poles inclined 25° to 55° from the loading direction. LCF life is dominated by crack propagation and we have shown that a correlation between the extent of facet formation and shorter LCF life. Since facets form only in the small crack and low- ΔK regimes, this implied that

Further, when clusters of grains that are capable of supporting faceted growth are present the LCF life is adversely affected. While there is more detailed work to be done and more data needs to be analyzed for consistency, we feel this way of analyzing the relation between microtexture and LCF life is very promising and

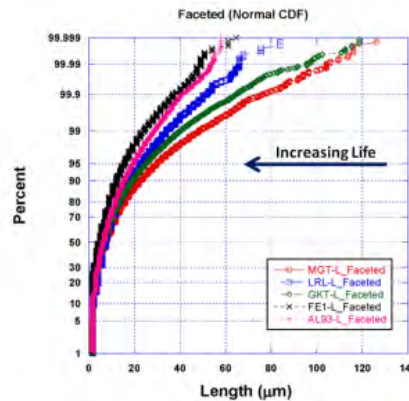


Figure 4. Cumulative distribution function showing time spent in facet forming orientations for six different conditions

Comment [rev13]: This needs to be replaced with a higher res image (still compressed in JPEG form) prior to submission. Andy should be sending this to Adam on Friday.

may be useful for pre-screening and ranking various microstructures. Naturally, some aspects of this analysis would have to be modified if the crack growth mechanism changes.

Acknowledgement

One of the authors (ALP) would like to acknowledge the support and encouragement of the AFRL management during the preparation of this manuscript.

REFERENCES

- 1) T.R. Bieler and S.L. Semiatin, Int. J. Plasticity, 2002, 18, pp. 1165-1189.
- 2) A.P. Woodfield, M.D. Gorman, R.R. Corderman, J.A. Sutcliffe and B. Yamrom, *Ti'95: Science and Technology*, Proc. 8th Int. Conf. Ti, P.A. Blenkinsop, W.J. Evans and H. Flower, eds., Inst. Materials, London, UK, pp. 1116-1123.
- 3) W.J. Evans and M.R. Bache, Int. J. Fatigue, 1994, 16, pp. 443-452.
- 4) E. Uta, N. Gey, P. Bocher, M. Humbert and J. Gilgert, J. Microscopy, 2009, 233:3, pp. 451-459.
- 5) V. Sinha, M.J. Mills and J.C. Williams, Met. Mater. Trans. A, 37, 2006, pp. 2015-2026.
- 6) A.L. Pilchak and J.C. Williams, Met. Mater. Trans. A, 42, 2011, pp. 1000-1027.
- 7) V. Hasija, S. Ghosh, M.J. Mills and D.S. Joseph, Acta Mat. 51, pp. 4533-4549.
- 8) G. Venkataramani, D. Deka and S. Ghosh, ASME, 2006, 128, pp. 356-365.
- 9) F.P.E. Dunne, A. Walker and D. Rugg, Proc. Roy. Soc. A, 2007, 463, pp. 1467-1489.
- 10) K. Kirane, S. Ghosh, M. Groeber and A. Bhattacharjee, J. Eng. Mat. Tech. 2009, 131, article 021003, pp. 1-14.
- 11) M.R. Bache, W.J. Evans and H.M. Davies, J. Mat. Sci. 1997, 32, pp. 3435-3442.
- 12) A.L. Pilchak, PhD Dissertation, The Ohio State University, 2009.
- 13) A.W. Bowen, Acta Metall. 1975, 23:11, pp. 1401-1409.
- 14) I. Bantounas, T.C. Lindey, D. Rugg and D. Dye, Acta Mater. 2007, 55, pp. 5655-5665.
- 15) A.L. Pilchak and J.C. Williams, Met. Mater. Trans. A, 2011, 42, pp. 773-794.
- 16) M.F.X. Gigliotti, B.P. Bewlay, J.B. Deaton, R.S. Gilmore and G.A. Salishchev, Met. Mater. Trans. A, 2000, 31, pp. 2119-2125.
- 17) C.M. Ward-Close and C.J. Beevers, Met. Trans. 1980, 11, pp. 1007-1017.